NON-PROPAGATING CRACKS UNDER IN-PHASE MODE I AND II LOADINGS

L. Susmel[1], D. Taylor[2]
[1]Department of Engineering - University of Ferrara
Via Saragat, 1 - 44100 Ferrara (Italy)
[2]Department of Mechanical and Manufacturing Engineering - Trinity College
Dublin 2, Dublin (Ireland)
E-mail: lsusmel@ing.unife.it, dtaylor@tcd.ie

Abstract

A number of fatigue tests have been performed on sharply notched specimens subjected to fully-reversed in-phase MODE I and II loadings. The material employed in this investigation was a commercial low carbon steel. The biaxial specimens were tested in the high-cycle fatigue regime in order to generate non-propagating cracks under mixed mode loadings. The detected non-propagating cracks were seen to be very long: independently of the degree of multiaxiality, their length ranged from 0.6mm up to 0.9mm, approximately. This result is very interesting, because it seems to strongly support the theory recently formulated by Taylor [1]: non-propagating cracks have a length which is of the order of 2L, where L is the material characteristic length [2]. Finally, it can be highlighted also that non-propagating cracks have been seen to grow along the direction experiencing, at a distance equal to L/2 from the notch tip, the maximum range of the normal stress. On the contrary, the early stage of the non-propagating crack formation was seen to be mainly mode II dominated: biaxial crack-paths showed a Stage 1-like and a Stage 2-like process, despite the fact that the tested notches were sharp and the stress fields in the vicinity of the notch tips were biaxial.

Introduction

Metal materials are characterised by a threshold value named “fatigue limit”. This reference value is very important in practical applications, because when a component is in fatigue limit condition failures should not occur up to a number of cycles to failure theoretically equal to infinity. From a scientific point of view, the fatigue limit condition results in the formation of a non-propagating crack (NPC) emanating from components’ weakest point. In plain specimens, the propagation of this crack is arrested by the first grain boundary (or by the first micro-structural barrier) [3]: this is the early stage of the micro/meso-crack initiation, and, according to Miller’s schematisation [4], it can be assumed to be the initial portion of Stage 1. On the contrary, in the presence of sharp notches, NPCs are much longer [5, 6] and their length mainly depends on the material fatigue properties [1, 7].

In particular, Yates and Brown [7] suggested that maximum NPC length is equal to:

$$a_0 = \frac{1}{\pi}\left(\frac{\Delta K_{th}}{F \cdot \Delta\sigma_0}\right)^2 \qquad (1)$$

where $\Delta\sigma_0$ is the plain fatigue limit, ΔK_{th} is the range of the threshold value of the stress intensity factor and, finally, F is the geometrical correction factor for the LEFM stress

intensity factor. Eq. (1) makes it evident that, according to Yates and Brown's model, NPC length depends both on the material fatigue properties and on the component geometry.

On the contrary, using different arguments, Taylor [1] suggested that NPC length should depend just on the material fatigue properties. In particular, the maximum NPC theoretical length was supposed to be equal to 2L, where L is the material characteristic length, defined as [2]:

$$L = \frac{1}{\pi}\left(\frac{\Delta K_{th}}{\Delta \sigma_0}\right)^2 \tag{2}$$

In the present study, sharply notched specimens were tested in the high-cycle fatigue regime in order to study the NPC paths under in-phase biaxial fatigue loading. The generated results were then used both to check whether the NPC length depends on the degree of multiaxiality and to verify the validity of the idea that crack propagation is characterised by the two classical stages also in the presence of sharp notches under biaxial fatigue loading. Finally, the critical planes predicted by two methods previously proposed by the Authors have been compared to the observed crack paths in order to better understand their connection to the physical reality.

Experimental details and results

The material employed in this investigation was a low carbon steel having the following mechanical properties: tensile strength σ_T=410 MPa, fully-reversed axial fatigue limit $\Delta\sigma_0$=338 MPa, range of the threshold value of the stress intensity factor ΔK_{th}=8.5 MPa $m^{½}$ (R=-1), material characteristic length L=0.2 mm, average grain size 18μm.

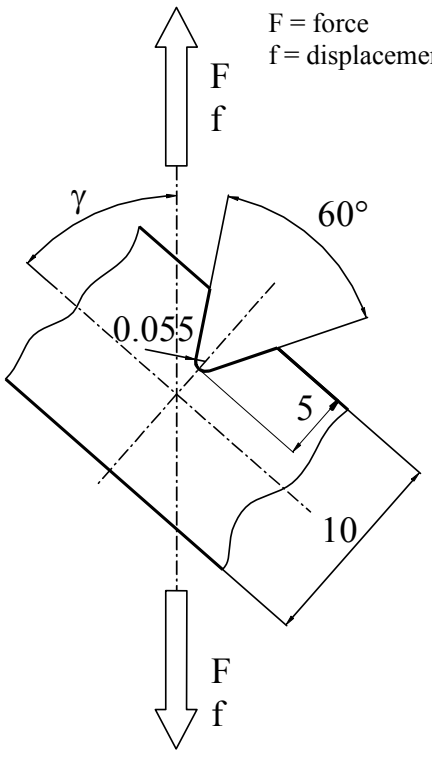

FIGURE 1. Notch geometry and symbolism (Dimensions in mm).

Samples were derived from the compact tension-shear specimens, replacing cracks with V-shaped notches having a nominal opening angle of 60° (Fig. 1) [8]. Different ratios between MODE I and II loadings were obtained by changing the γ angle value. In particular, specimens having γ angle equal to 90°, 60°, 45° and 0°, respectively, have been tested.

The experimental procedure was similar to the one used by Frost [5, 6] to generate non-propagating cracks in notched cylindrical specimens under rotating bending.

Initially, for every γ angle value investigated, some calibration tests were performed in the high cycle fatigue regime (form $3\cdot10^5$ cycles up to $8\cdot10^6$ cycles) to define a reference fatigue strength at 10^7 cycles to failure. The generated fatigue data are plotted in the diagrams of Fig. 2, whereas the synthesis of the experimental results are summarised in Tab. 1. In particular, this table reports: the code of the data series; the inverse slope of the fatigue curve, k; the reference force amplitude, F_A, extrapolated at 10^7 cycles to failure, and the crack path described according to the schematisation sketched in Fig. 4.

TABLE 1. Synthesis of the experimental results.

Series	k	F_A / kN	L_I / mm	ϕ_I / °	L / mm	ϕ_{II} / °
90_05	12.5	1.26	0.160	10.1	0.89	34.4
60_05	8.6	1.00	0.100	37.7	0.62	49.9
45_05	11.5	1.01	0.092	17.5	≈4	41.1
0_05	6.1	1.00	0.021	21.2	0.74	≈0

The statistical re-analyses of the fatigue results were performed under the hypothesis of a log-normal distribution of the number of cycles to failure, with a confidence level of 95%.

The tested specimens were definitively thick: the thickness was equal to 5mm. Therefore, to force cracks to initiate and grow only on the specimen surface, notches were machined using a particular device: the used tool allowed us to have a notch root radius of about 0.055 mm on one surface, whereas the notch root radius on the other surface was equal to about 0.1 mm. Finally, it can be highlighted that the fatigue cracking process involved a couple of grains in the thickness direction, so that cracks grew under plane stress.

In order to check if the detected crack was a non-propagating one, tests were stopped at $1.2 \cdot 10^7$ cycles and then the crack length was measured. Subsequently, these specimens were tested again up to $1.5 \cdot 10^7$ cycles. If the detected crack did not increase its length, it was assumed to be a non-propagating one. Following this procedure, non-propagating cracks were generated under different ratios between MODE I and II loadings. The lengths of the detected NPC are summarised in Tab. 1. Finally, it can be highlighted that the crack detected at $1.5 \cdot 10^7$ for the 45_05 configuration was not a NPC.

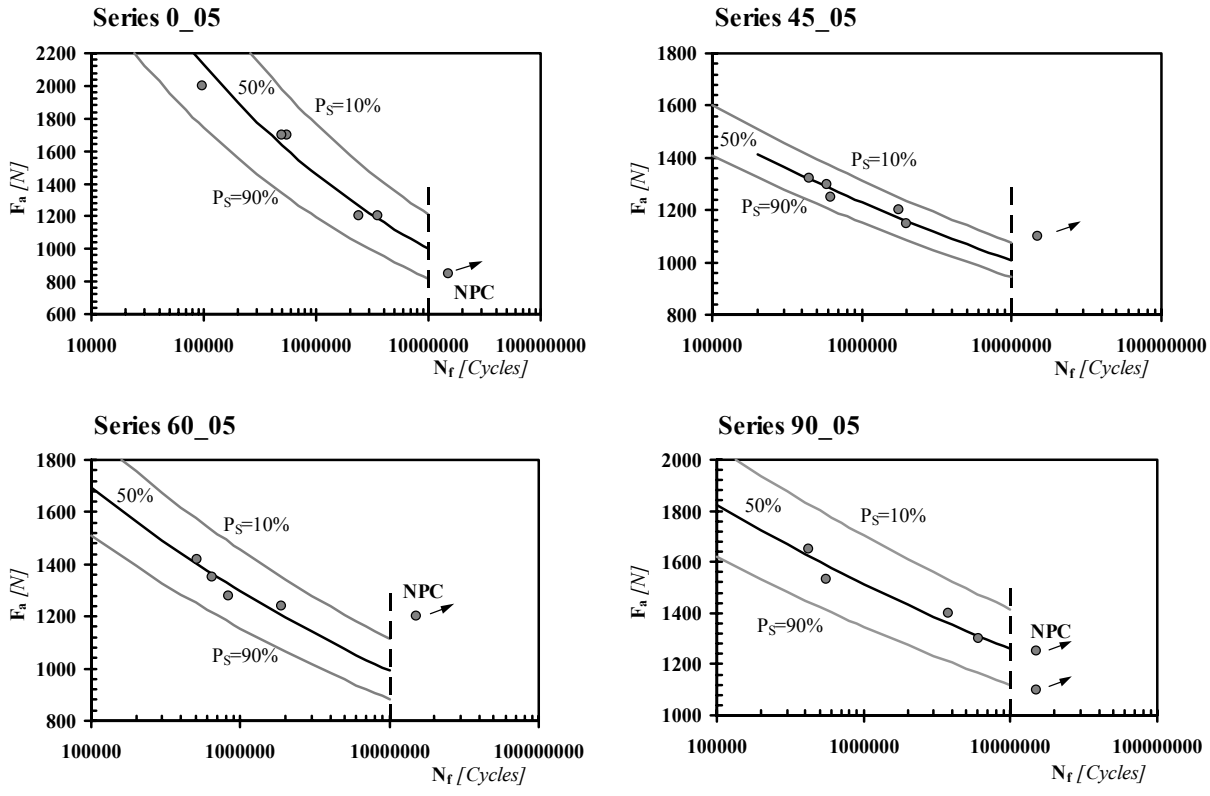

FIGURE 2. Fatigue results.

The material cracking behaviour was investigated by polishing the cracked specimens up to a mirror-like finish. Subsequently, surfaces were etched to study the grain distribution in the fatigue process zone. Fatigue crack paths were then inspected by using a LEICA MEF4M microscope with a JVC TK-C1380 digital camera. Pictures and measurements were managed using the A4i Docu software.

Two fatigue damage models

Recently, the Authors proposed two methods suitable for predicting the high-cycle fatigue strength of sharply notched components under multiaxial fatigue loading [8]. These two methods were seen to be successful, giving predictions laying within an error interval of about 15% independently of the degree of multiaxiality.

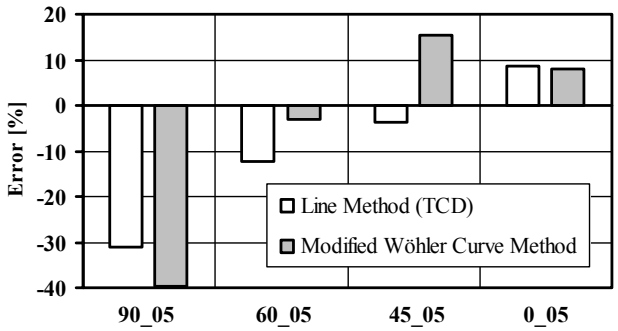

FIGURE 3. Methods accuracy in predicting the multiaxial fatigue limits of the tested specimens.

This result is very interesting, because the two methods make quite different assumptions on the parameters controlling fatigue damage.

In particular, Taylor's Theory of Critical Distances (TCD) [2, 8] postulates that the critical path is the one experiencing the maximum normal stress range. This assumption takes as its starting point the idea that: (i) propagation is the most important stage in formation of NPCs; (ii) NPC growth is mainly mode I dominated.

On the contrary, Susmel's Modified Wöhler Curve Method (MWCM) [8, 9] assumes that the initial (Stage 1) crack propagation is the critical stage in determining the fatigue limit. According to this method, fatigue limit estimations must be performed considering the stress components relative the plane experiencing the maximum shear stress amplitude. This plane must be determined considering the stress state calculated at a distance from the tip of the stress concentrator equal to L/2 [9].

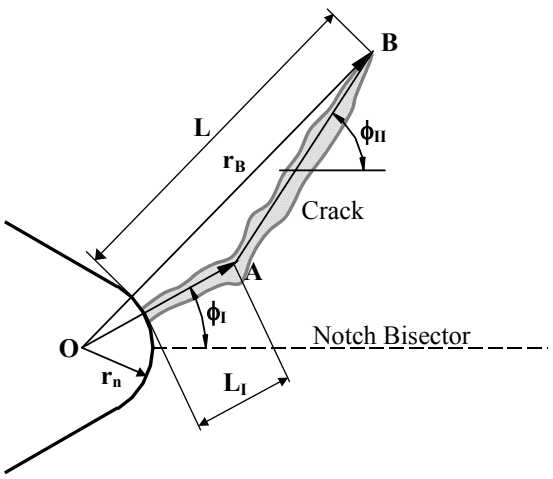

FIGURE 4. Schematisation adopted to measure the crack path orientation.

The error diagram reported in Fig. 3, obtained considering the fatigue results summarised in Tab. 1, again confirms the accuracy of our methods, even though they are founded on different assumptions (see Ref. [8] for the in field application of the aforementioned methods). The highest error was obtained by both methods when they were used to predict the high-cycle fatigue strength of the 90_05 configuration. This could be a consequence of the fact that this configuration was the most critical one, because the gauge length was perpendicular to the applied load. Moreover, a secondary bending was always present, resulting in an increase of the data scattering.

In the next section, the validity of the assumptions on which our methods are based will be compared to the observed cracking behaviour of the tested specimens.

Non-propagating cracks and fatigue damage models

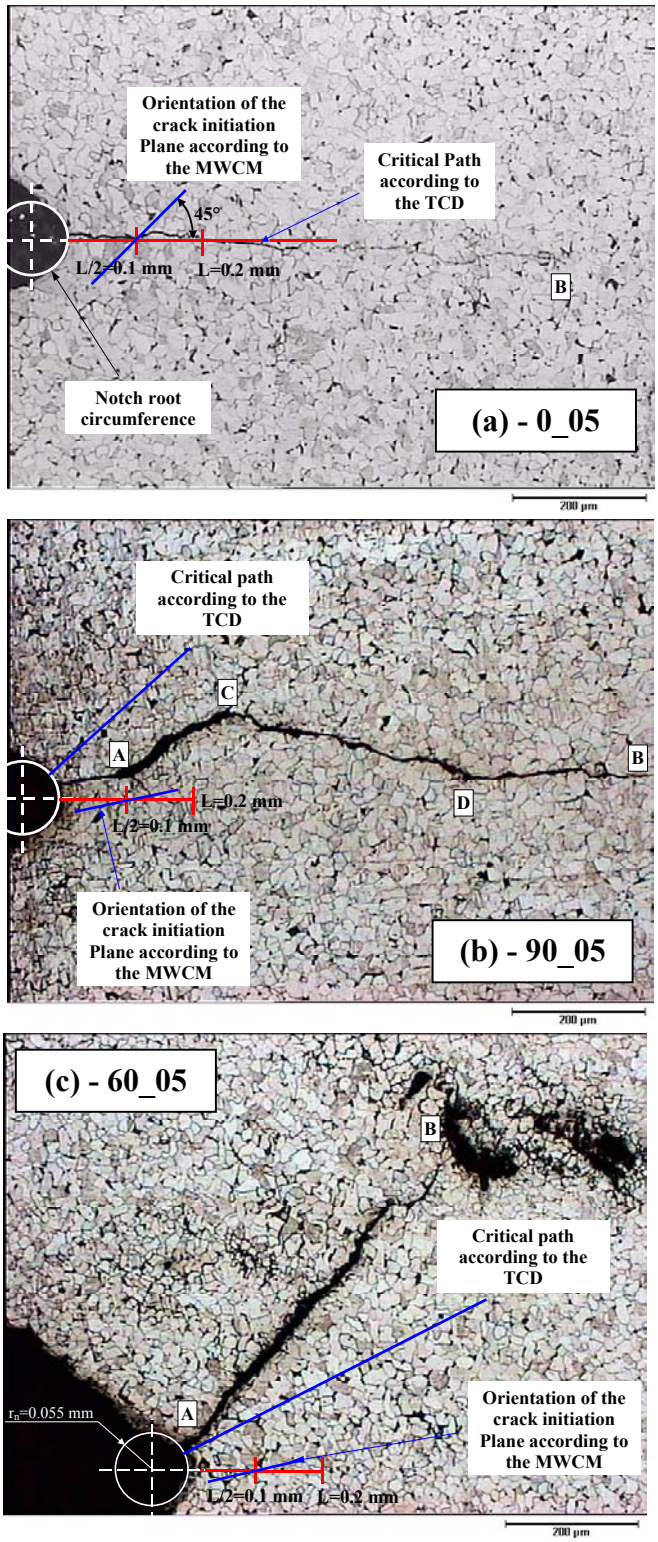

FIGURE 5. Detected Non-Propagating cracks.

Initially, attention can be focused on the measured NPC lengths. Table 1 shows that the average length of the generated NPCs was equal to 0.75 mm.

Uniaxial notched specimens were characterised by a geometrical correction factor, F, equal to 2.8 [10]. According to Eq. (1), the length of the NPCs should have been equal to 0.027 mm. On the contrary, according to Taylor's hypothesis - Eq. (2), the length of the NPCs should have been equal to 2L=0.4 mm. This makes it evident that, in the studied cases, both models were not capable of satisfactorily predicting the NPC length. In any case, Taylor's method gives a closer approximation to the NPC length but there is still some error: the average length is closer to 4L than to 2L. This discrepancy could be a consequence of the fact that, due to the notch geometry, cracks were forced to initiate and grow on the surface and not at that specimen section experiencing the maximum plane strain condition.

The pictures of the generated NPCs are reported in Fig. 5, whereas crack path orientations are summarised in Tab. 1. The orientation of the critical planes reported in Fig. 5, calculated according to the two methods reviewed above, have been determined by FE linear-elastic models and assuming an average value of the notch root radius equal to 0.055mm.

Fig. 5a shows that, under uniaxial fatigue loading, crack propagation was definitively mode I dominated. Moreover, as shown by Tab. 1, Stage 1 length covered two small grains at the crack initiation point. In this case, the TCD theory correctly predicted the position of the crack path (See Tab. 2 for a direct

comparison among the crack paths angles, ϕ_I and ϕ_{II}, and the critical path orientation predicted by our methods). For the 90_05 configuration (Fig. 5b), the MWCM accurately predicted the orientation of the Stage 1 plane, whereas the TCD correctly estimated the orientation of the Stage 2 plane. Finally, Fig. 5c shows that for the 60_05 configuration, the two methods predicted the orientation of the two Stages with an acceptable approximation.

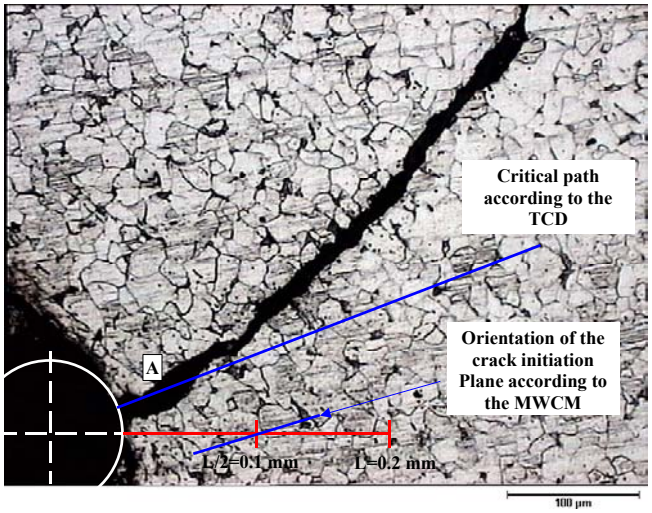

FIGURE 6. High-cycle fatigue cracking behaviour of the 45_05 configuration.

The picture reported in Fig. 6 shows the crack detected in a 45_05 specimen at $1.5 \cdot 10^7$ cycles to failure. This crack was not an NPC, but it has been reported here because it is representative of the high-cycle fatigue cracking behaviour of this specimen configuration. Fig. 6 proves again that the MWCM correctly predicted the orientation of the Stage 1 plane and that the TCD estimated the orientation of the Stage 2 plane with an acceptable error.

In the previous paragraphs, it was always implicitly assumed that a Stage 1-like process was present.

TABLE 2. Experimental and predicted orientation of the two Stages.

		MWCM		TCD
Series	ϕ_I / °	ϕ / °	ϕ_{II} / °	ϕ / °
90_05	10.1	12.8	34.4	42
60_05	37.7	13.1	49.9	27
45_05	17.5	17.8	41.1	21
0_05	21.2	45	≈0	0

The validity of this assumption seems to be strongly supported by the stress-distance curves reported in Fig. 7. These diagrams have been built by plotting, along the measured biaxial crack paths, the normal and tangential stress determined by linear-elastic FE analyses. Fig. 7 shows that the shear stress contribution was never negligible up to point A (Stage 1-like process). On the contrary, the subsequent propagation (A-C in Fig. 7a and A-B in Fig. 7b) was mainly mode I dominated, that is, the normal stress contribution prevailed over the one due to the tangential stress (Stage 2-like process).

This result is very interesting, because it seems to strongly support the idea that crack paths are characterised by the two classical Stages [4] both in the presence of sharp notches and under multiaxial fatigue loading.

Finally, observing the L_I values reported in Tab. 1, it can be noticed that Stage 1 length increased as the contribution of shear stress components to the fatigue damage increased.

This results seems to confirm the fact that the material characteristic length under shear stress is larger than under uniaxial fatigue loading [11].

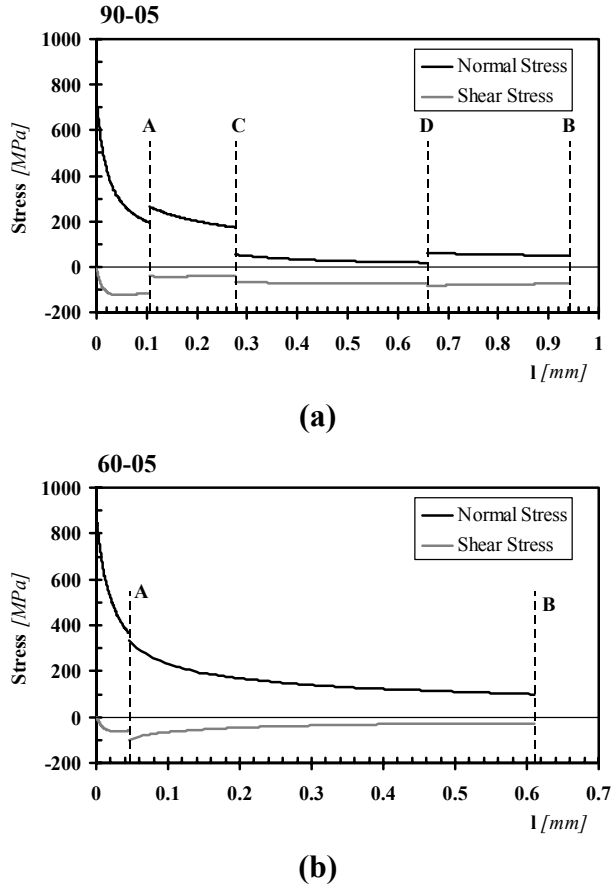

FIGURE 7. Linear-elastic stresses along the NPC paths detected in 90_05 (a) and 60_05 (b) configuration..

Discussion

The high-cycle fatigue behaviour showed by the tested specimens confirmed the fact that crack paths are characterised by the two classical stages also under mixed mode loading: the Stage 1-like process is mainly shear stress dominated, whereas the Stage 2-like process is mainly mode I governed.

According to the hypotheses on which they are based, the MWCM and the TCD seem to correctly model crack initiation and crack propagation, respectively.

It is important to highlight here that these two methods are just engineering tools developed to assess components in situations of practical interest and not "scientific" methods suitable for rigorously predicting crack path directions. In particular, these methods are based on the calculation of the linear-elastic stress fields in the vicinity of the stress concentrators. This aspect is very important, because it makes them suitable for being used by post-processing FE linear-elastic results, reducing time and costs of the design process.

The main limitation in using our methods for predicting crack paths depends on the fact that the fatigue limit estimation in un-cracked bodies is mainly a short-crack problem. The propagation phenomenon of short-cracks depends on two primary factors [9, 12]: grain plasticity and material morphology close to the stress concentrator apex. Unfortunately, accounting for these two aspects would be impossible in industrial reality: prediction methods would be too cumbersome to be applied.

It is evident now that our methods represent just two sound compromises between the necessity of rigorously modelling the physical processes taking place in the fatigue process zone and the necessity of having simple methods to easily be managed in practical situations.

Conclusions

1) The length of the detected NPCs is of the order of 4L, independently of the degree of multiaxiality;

2) In the presence of sharp notches subjected to biaxial in-phase loading, crack paths are characterised by a Stage 1-like and a Stage 2-like process;

3) Taylor's TCD and Susmel's MWCM proved to be linked to the physical reality: the use of linear-elastic stresses make them accurate enough to correctly predict the fatigue limit under any kind of fatigue loading;

4) Further work also needs to be done in this area to investigate NPCs behaviour under out-of-phase multiaxial fatigue loadings.

References

1. Taylor, D, *Fatigue Fract. Engng. Mater. Struct.*, vol. **24**, 215-224, 2001.
2. Taylor, D., *Int. J. Fatigue*, vol. **21**, 413-420, 1999.
3. Akiniwa, Y., et al., *Fatigue Fract. Engng. Mater. Struct.*, vol. **24**, 817-829, 2001.
4. Miller, K. J., *Fatigue Fract. Engng. Mater. Struct.*, vol. **16**, 931-939, 1993.
5. Frost, N. E., *In Proc. Inst. Mech. Engrs.,* Vol. **173**, 811-834, 1957.
6. Frost, N. E., *Aeoronaut. Quart.* **VIII**, 1-20, 1957.
7. Yates, J. R., Brown J. R., *Fatigue Fract. Engng. Mater. Struct.*, vol. **10**, 187-201, 1987.
8. Susmel, L., Taylor, D., *Fatigue Fract. Engng. Mater. Struct.*, vol. **26**, 821-833, 2003.
9. Susmel, L., *Fatigue Fract. Engng. Mater. Struct.*, vol. 27, 391-411, 2004.
10. Tada, H., Paris, C. P., Irwin, R. G., *The Stress Analysis of Cracks – Handbook*. Professional Engineering Publishing, Bury St. Edmunds, UK (Third Edition), 2000.
11. Susmel, L., Taylor, D., The theory of critical distances to predict the high-cycle fatigue strength of notched components under torsional loading. Submitt. to *Int. J. Fatigue*, 2004.
12. Tomkins, B., *Philosophical Magazine*, 1041-1066, 1968.